# Cellulose nanocrystal stabilized beeswax dispersions for consolidation of encaustic paintings

Citation for the original published paper (version of record):

Jia, Y., Henrik-Klemens, Å., Persson, M. et al (2025). Cellulose nanocrystal stabilized beeswax dispersions for consolidation of encaustic paintings. International Journal of Biological Macromolecules, 312. http://dx.doi.org/10.1016/j.ijbiomac.2025.144085

International Journal of Biological Macromolecules 312 (2025) 144085

Contents lists available at ScienceDirect

International Journal of Biological Macromolecules

journal homepage: www.elsevier.com/locate/ijbiomac

# Cellulose nanocrystal stabilized beeswax dispersions for consolidation of encaustic paintings

Yiming Jia [a], Åke Henrik-Klemens [b], Michael Persson [c], Krister Holmberg [a], Romain Bordes [a,*]

[a] Department of Chemistry and Chemical Engineering, Chalmers University of Technology, 412 96 Gothenburg, Sweden
[b] FibRe – Centre for Lignocellulose-based Thermoplastics, Department of Chemistry and Chemical Engineering, Chalmers University of Technology, 412 96 Gothenburg, Sweden
[c] Chalmers Industriteknik, 412 58 Gothenburg, Sweden

ARTICLE INFO

*Keywords:*
Pickering emulsion
Painting consolidation
Hydrophobic

ABSTRACT

We present formulations of dispersions based on beeswax for consolidating encaustic paintings, which use beeswax as a binder and are applied on a canvas or wooden substrate. Commercial natural and synthetic adhesives are used for consolidation of such paintings, but they often have problems due to the consolidant material not being compatible with the original painting. The dispersions were prepared by combining Pickering beeswax emulsions stabilized by cellulose nanocrystals (CNC) with hydrophobically modified ethylhydroxyethylcellulose (EHM). The drop size of the emulsion varied with the beeswax content and the emulsion drops displayed inclusions of water droplets. These inclusions led upon drying to films that showed a hollow micromorphology, which enhanced the water evaporation, giving high breathability. The dispersions comprising beeswax, CNC and EHM were stable over time and the viscosity was governed by the amount of EHM in the formulation. The dried films were very hydrophobic with a water contact angle of about 130°. The emulsion-based formulations were tested on encaustic painting mock-ups made on wood substrate to examine their adhesive strength and water resistance. The formulations achieved better performance than commercial products used as consolidants for encaustic paintings. The beeswax-based compositions, which contain only green components and free of volatile organic compounds, offer an interesting platform for consolidation in the field of cultural heritage.

## 1. Introduction

Environmental changes, such as temperature and moisture fluctuation, or chemical processes resulting from the adsorption of volatile pollutants can give rise to severe degradation of work of arts, such as delamination, cracking, and ultimately flaking of paint artworks [1,2]. A common treatment, consolidation, is therefore often needed. It consists of the deposition of a suitable material, often a polymer, on top of cracked or flaking layers of painted surfaces. This treatment is one of the most delicate operations because it may be invasive from chemical and aesthetical points of view and there are therefore severe criteria regarding the performance of consolidants [3].

Historically, a variety of natural adhesives, such as animal glue, wax, starch and resin, have been used for consolidation of paintings; however, the often-poor stability and low performance reported have limited their application [4]. Synthetic adhesives were introduced during the 20th century as a substitute for natural adhesives for consolidation of deteriorated paintings. These adhesives are homo- or copolymers based on common monomers such as vinyl acetate, acrylate, methacrylate and ethylene [5]. However, such polymeric adhesives tend to form a coating layer, i.e. a film, that prevents the migration of soluble salts and moisture, which may lead to severe damage to the artworks [6,7]. Moreover, their incompatibility with the original substrate often results in poor long-term stability and strong mechanical stress that can cause further deterioration. In an attempt to overcome these problems combinations of natural and synthetic adhesives have been used for consolidation; however, with limited success [8]. Relatively few efforts have been made to develop consolidating adhesives specifically for the field of cultural heritage [9]. However, over the past two decades, nanotechnology has emerged at the forefront of the development of innovative solutions for the restoration and conservation of works of art [10], showing promising results in cleaning [7], deacidification [11], consolidation [12] and microbial control [13] on various artefacts, such as stone [14], paintings [15,16], paper [17–19], leather [20] and wood

---

* Corresponding author.
*E-mail address:* bordes@chalmers.se (R. Bordes).

https://doi.org/10.1016/j.ijbiomac.2025.144085
Received 27 January 2025; Received in revised form 28 April 2025; Accepted 8 May 2025

[21]. Nanocellulose has been proposed as a novel consolidant for historical papers and canvases [22,23]. It has many attractive features such as excellent mechanical properties and a large surface area. In addition, it is renewable and biodegradable, and it is, by nature, compatible with artworks containing cellulose [24].

Wax, both natural and synthetic, is commonly found in various historical collections. Encaustic paintings are examples of wax artefacts. These are composed of a paint with beeswax as binder applied to a canvas or to a wooden object or a wall [25]. Beeswax is a complex hydrophobic material containing many constituents, including long-chain hydrocarbons, fatty acids, fatty alcohols, and esters of long-chain acids and alcohols [26]. Waxes are sensitive to many solvents, they are malleable and susceptible to damage by heat and pressure. In addition, they often display white surface bloom, and they can become hard and brittle with aging [27].

The traditional hot-melt wax application method is risky for paintings because an increase in temperature and/or pressure may distort the painting and the adhesive may penetrate in an uncontrollable way, which might permanently darken the surface [28]. When BEVA® 371 was developed, it has proven to counteract effectively these issues. It has therefore been widely used for conservation of works of art. It is composed of paraffin wax, poly (ethylene-vinyl acetate) and aromatic hydrocarbons and has been found to improve the bonding capacity. In addition, its penetration is limited. However, the heating and toxicity issues remain a challenge for BEVA [29,30]. Thus, the field is still searching for novel consolidation strategies based on eco-friendly materials to fulfill current practice requirements. Ideally the material should present material similarities with both substrate and wax. In that context, formulation of emulsions of wax may have appealing features.

Pickering emulsions, i.e., particle stabilized emulsions, have received considerable attention lately because of their higher stability, lower toxicity, and better stimuli-responsiveness, compared with emulsions that are stabilized by surfactants [31,32]. Recently, Pickering emulsions with halloysite nanotubes as stabilizing particles have been applied for cleaning and consolidation of cultural heritage [33,34].

Cellulose nanocrystals (CNCs) are bio-sourced nanoparticles that can stabilize emulsions through the Pickering mechanism [35]. We have previously used CNCs to produce Pickering emulsions of paraffin wax for fabrication of continuous filaments [36]. To the authors' knowledge, up to now CNC has not been used to make Pickering emulsions of wax for conservation of culture heritage.

The development of tailored consolidants for art objects based on renewable natural sources can be regarded as a sustainable route, provided the new materials cope with the specific requirements [16].

In the work presented here, we prepared and evaluated a Pickering emulsion of beeswax with a cellulose ether added to increase the viscosity and with CNC as stabilizing nanoparticles. As cellulose ether, we used Bermocoll® EHM (called only EHM in the following), which is a hydrophobically modified ethylhydroxyethylcellulose, known to increase the viscosity in paint formulations through self-association and through interaction with surfactant micelles [37,38]. In the present formulation there are no surfactants; instead, the hydrophobic side chains of EHM will interact with the hydrophobic beeswax/CNC microparticles, thus forming a network in the dispersion. The viscosity can be adjusted by the content of EHM and beeswax/CNC. Moreover, the dispersion forms a highly hydrophobic layer with hierarchical structure after drying, making it an ideal material as adhesive for flaking encaustic paintings. It is noteworthy that all the ingredients in the dispersion, beeswax, cellulose nanocrystals and a cellulose ether, are green and compatible with encaustic artefacts, thus representing a promising alternative material to natural and synthetic polymers in the cultural heritage conservation field.

## 2. Materials and methods

### 2.1. Materials

Cellulose nanocrystals (CNC) were obtained from CelluForce, Canada. Red ocher pigment and beeswax (bleached) were purchased from Kremer Pigmente GmbH & Co. Bermocoll® EHM 200 (Hydrophobically modified EHEC) was obtained from Nouryon, Sweden. The Masonite sheet with 3 mm thickness was purchased from Creative Deco. Calcium chloride dihydrate (98 %), the fluorescence dye Rhodamine B and Whatman filter paper were purchased from Sigma-Aldrich, Sweden. Poly(2-ethyl-2-oxazoline) with M.W. 500,000 (Aquazol® 500) was purchased from Thermo Scientific, Sweden.

### 2.2. Preparation of green consolidants

Beeswax Pickering emulsions with CNC as stabilizing agent, in presence of $CaCl_2$, were prepared at 80 °C with a high-speed homogenizer (Heidolph Instruments, 10 mm shaft) operating at 15000 rpm for 2 min. In brief, beeswax20/CNC1 was prepared by dispersing 4 g of beeswax (20 wt%) in 16 g of 1 % CNC dispersion with 4.7 mg of $CaCl_2$. Other formulations followed the same procedure with different ratios. The microspheres were characterized after cooling to room temperature. Various concentrations of EHM (0.2 %–3 %) were also added to the emulsions at ambient temperature, the prepared formulations were listed in Table S1.

### 2.3. Preparation of encaustic painting mockups

500 mg of red ocher was mixed with 5 g of natural unbleached beeswax that had been melted at 85 °C in a glass vial. The hot mixture was spread on a preheated pan-shaped parchment paper, creating a smooth surface, which was cooled to room temperature to give a paint layer about 1 mm thick that was cut into 1 × 1 cm pieces. The beeswax bonding area was prepared by applying 15 mg of beeswax to the heated Masonite onto which the paint layer was applied and lightly pressed. A similar procedure was carried out with the other consolidants. The mockups were then immersed in a petri dish filled with Milli-Q water and observed for 13 days.

### 2.4. Characterization

Fluorescence microscopy, laser diffraction analysis, scanning electron microscopy, viscometry, UV–Vis spectroscopy, tensiometry, ATR-FTIR, thermogravimetric analyses and measurement of water vapor transmissions were performed to characterize the Pickering emulsions and consolidants. Tensile measurements, colorimetry and dynamic mechanical analysis were performed to evaluate the consolidation efficiency. The details of the preparation of the test samples and instrument parameters are given in supporting information.

## 3. Results and discussion

### 3.1. Characterization of the Pickering emulsions

The green dispersion designed for consolidation of deteriorated encaustic paintings is schematically shown in Fig. 1. The CNC used has a diameter of 7.5 ± 2.8 nm and a length of about 500 nm [23]. The Zeta potential of the CNC dispersion was tested at different pH values and remained stable between pH 2 and 12 (Fig. S1a). The contact angle of the CNC dry film is 49° (Fig. S1b). The 1 % CNC dispersion exhibited a viscosity of 2.5 cP. The beeswax microspheres stabilized by CNC will ensure compatibility with the painting's original wax binder and EHM was hypothesized to provide additional adhesion strength. After drying, over 80 % of the composite is made up of the Pickering emulsion, in which the beeswax content is the highest. The influence of beeswax

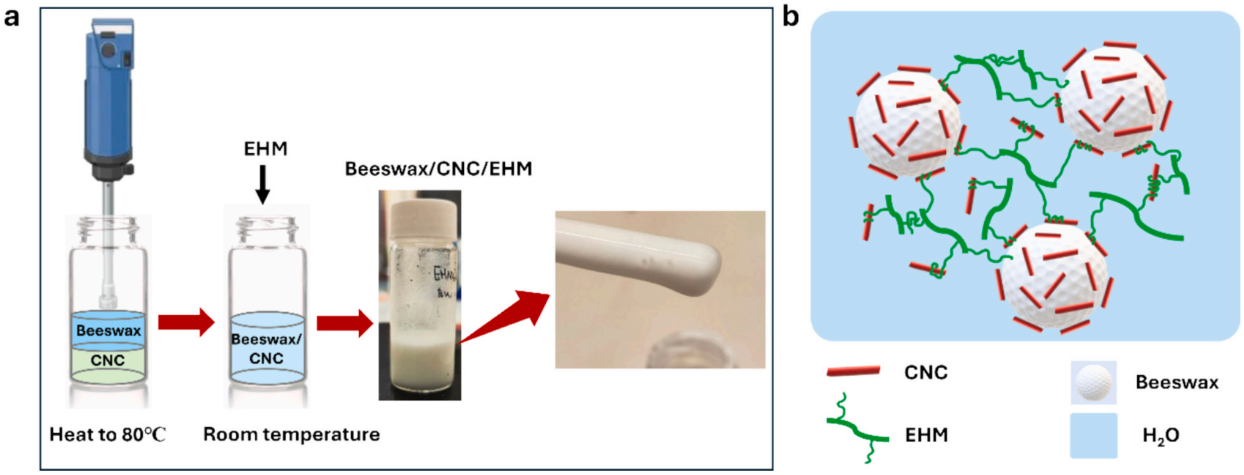

**Fig. 1.** Schematic illustration of (a) preparation and (b) structure of the beeswax/CNC/EHM dispersions.

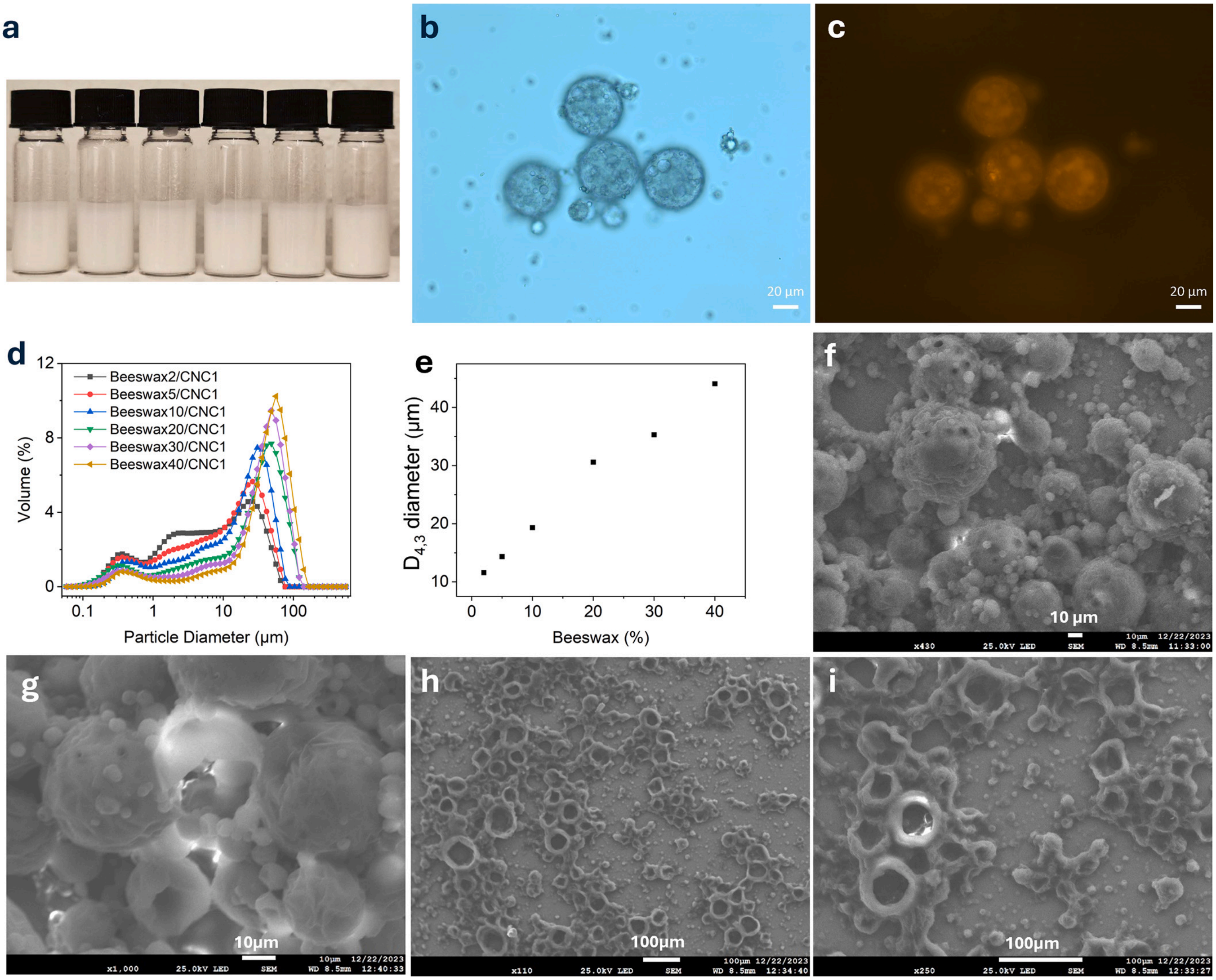

**Fig. 2.** (a) Pickering emulsions with 1 % CNC and 2, 5, 10, 20, 30, 40 % beeswax (from left to right); micrograph of Rhodamine B stained beeswax20/CNC1 emulsion: (b) bright field and (c) fluorescence microscopy; (d) laser diffraction of emulsions with 1 % CNC and 2–40 % beeswax; (e) $D_{4,3}$ diameter changes with beeswax contents; SEM image of beeswax20/CNC1/EHM1 coating: (f, g) before and (h, i) after heating at 85 °C for 15 min.

concentration on the droplet size in the emulsions was first investigated. Fig. 2a shows the appearance of Pickering emulsions stabilized by 1 % CNC and with the weight percentage of beeswax varied from 2 to 40 %. The Pickering emulsions remain stable regardless of the beeswax concentration. Fig. S2 shows optical microscopy images of the Pickering emulsions. As can be seen, the emulsion drops are spherical and seem to contain tiny spherical inclusions. The droplet size increases significantly with increasing concentration of beeswax. Rhodamine B was used to stain the emulsion containing 20 % beeswax and 1 % CNC. As shown in Fig. 2b and c, fluorescence microscopy images confirm the presence of droplet inclusions in the emulsion drops.

The size distribution of the drops of the Pickering emulsions was analyzed by laser diffraction. As seen in Fig. 2d and e, all the emulsions display a trimodal drop size distribution with the first peak centered at 0.1–1 μm, the second peak centered at 1–10 μm, and the third and the most intense peak centered above 10 μm. The drop distribution is broad, and the beeswax concentration significantly affects the distribution. The average drop size increased from 11 to 44 μm with an increase in beeswax content. The emulsion with 20 % beeswax and stabilized by 1 % CNC was chosen for more in-depth investigations as a consolidant due to its medium size and relatively homogeneous particle size distribution. This formulation is referred to as beeswax20/CNC1. Fig. 1a shows the appearance of this emulsion with 0.5 % EHM added (beeswax20/CNC1/EHM0.5). It displays a creamy and sticky texture. Fig. S3 shows the appearance of consolidants after drying on glass slides. The dry layer gives a white translucent surface with no glare. As the beeswax concentration decreases, the transparency of the consolidant increases. It is essential that the treatment of historical artefacts does not negatively impact their aesthetics. Application of the beeswax/CNC/EHM formulations for consolidation of cracked and flaking surfaces seems not to have a negative impact on the appearance of the painting surface.

SEM (scanning electron microscopy) images of beeswax20/CNC1 and beeswax20/CNC1/EHM1 are shown in Figs. S4 and 2f and g, respectively. It can clearly be seen that the dry films exhibit microspheres and small pores in a wide variety of shapes and sizes. The broken microsphere shown in Fig. 2g reveals its hollow nature. Fig. 2h and i shows the dry beeswax20/CNC1/EHM1 after heating. The beeswax has melted and become compressed, forming a porous structure, which confirms the hollow structure of the microspheres. Such a porous layer may be more breathable than the films from conventional polymeric consolidants.

### 3.2. Characterization of the consolidant film

ATR-FTIR (attenuated total reflectance – Fourier-transform infrared spectroscopy) was applied to characterize the beeswax20/CNC1/EHM1 dispersion after drying, as shown in Fig. 3. The characteristic bands of beeswax were identified at 2917 and 2849 cm$^{-1}$, corresponding to $CH_3$ and $CH_2$ stretching, 1737 cm$^{-1}$ for ester C═O stretching, 1473 and 1463 cm$^{-1}$ for C—H scissoring, 1170 cm$^{-1}$ for C—H bending, and 730 and 720 cm$^{-1}$ for C—H rocking [39]. Additionally, a weak broad band around 3350 cm$^{-1}$ was observed, which was attributed to O—H stretching from CNC and EHM. Due to the overlap between the absorptions of beeswax and cellulose based material around 1050 cm$^{-1}$, the C—O stretching of CNC and EHM was difficult to identify. However, the presence of CNC and EHM was evidenced by the increased intensity of vibrations in this region. No new absorption bands were detected in the composite, indicating that the combination of the components was achieved solely through physical interactions.

TGA (thermogravimetric analysis) was applied to further characterize the beeswax20/CNC1/EHM1 dispersion after drying. As shown in Fig. 4, a slight water weight loss was observed on both CNC and EHM in the range 30–100 °C. For CNC, cellulose decomposition led to a significant weight loss of 66.5 % between 250 and 400 °C, with a maximum degradation temperature of 306 °C and a residual ash content of 18.4 % [40]. In the case of EHM, backbone decomposition resulted in a 78.7 % weight loss within the 250–450 °C range, reaching a maximum degradation temperature of 360 °C and leaving a residual ash content of 11.3 %. Beeswax exhibited an initial weight loss around 220 °C, completing vaporization by 450 °C due to hydrocarbon decomposition, with a maximum degradation temperature observed at 402 °C. The DSC analysis shown in Fig. S5 revealed a solid-liquid phase transition at 62 °C [41]. As expected, the weight loss curves for beeswax20/CNC1, beeswax20/CNC1/EHM1 and beeswax20/CNC1/EHM2 closely aligned with that of plain beeswax, with maximum degradation temperatures in the range 395–402 °C. The influence of CNC and EHM on the thermal stability of composites is minimal due to their low content in composites.

The wettability of the emulsion-based consolidant layer was assessed by measuring contact angle on a glass slide. Initially, the surface layer from beeswax20/CNC1 emulsions with a weight percentage of added EHM of 0.0 %, 0.2 %, 0.5 %, 1.0 %, 2.0 % and 3.0 % were investigated. Only EHM at 1 %, 2 % and 3 % were included as references. As shown in Fig. S6, the layers formed by only EHM are highly hydrophilic with a

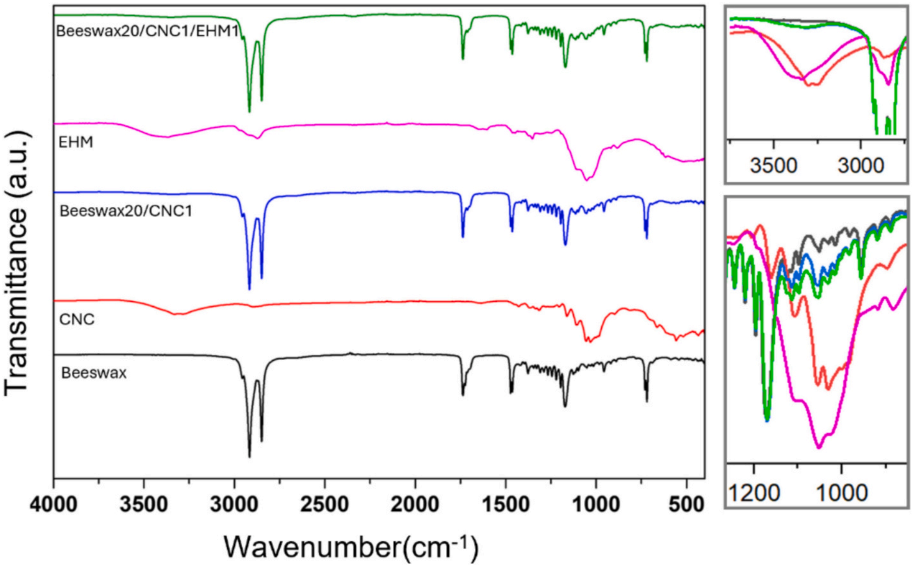

**Fig. 3.** ATR-FTIR spectra of beeswax20/CNC1/EHM1, EHM, beeswax20/CNC1, CNC and beeswax.

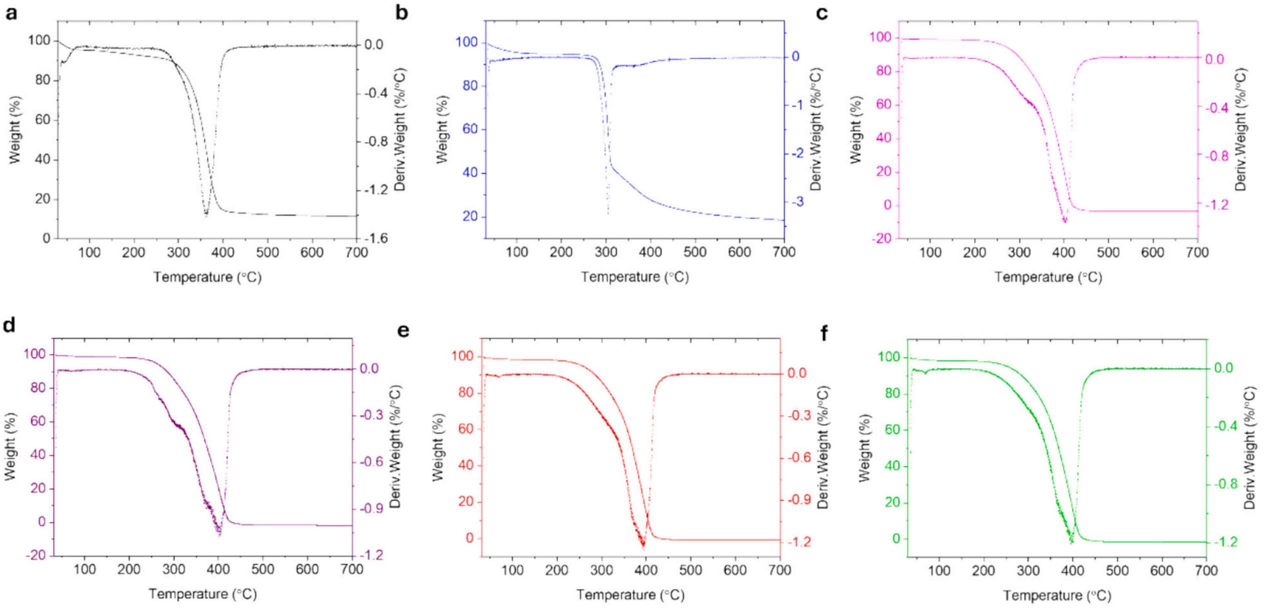

**Fig. 4.** TGA (solid) and corresponding DTGA (dash) curves of (a) EHM (black), (b) CNC (blue), (c) beeswax (pink), (d) beeswax20/CNC1 (purple), (e) beeswax20/CNC1/EHM1 (red) and (f) beeswax20/CNC1/EHM2 (green).

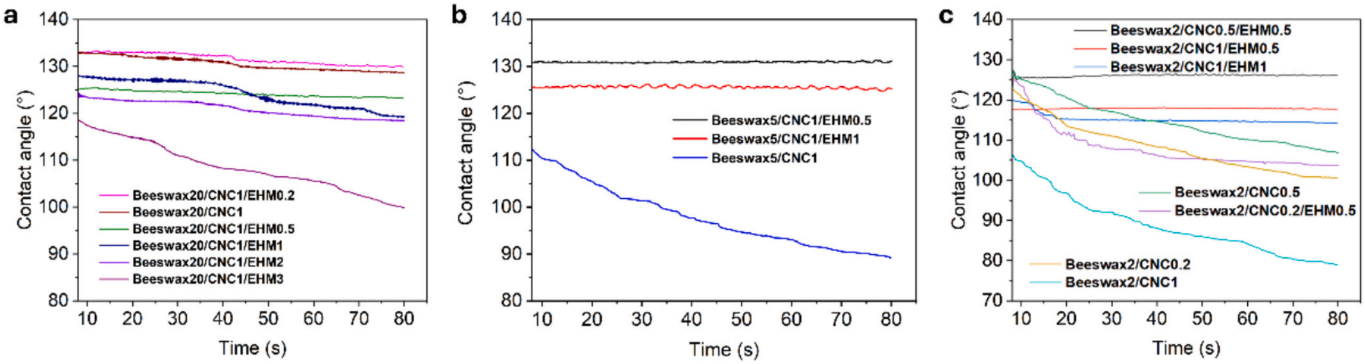

**Fig. 5.** (a) Contact angle measurements of the formulations with 20 % beeswax; (b) formulations with 5 % beeswax; (c) formulations with 2 % beeswax.

water contact angle of around 20°. The formulation without EHM, i.e. beeswax20/CNC1, is very hydrophobic giving a contact angle of about 130° (Fig. 5a). A formulation with a small amount of added EHM, beeswax20/CNC1/EHM0.2, gives approximately the same high contact angle while increasing amounts of EHM in the formulation results in progressively decreasing contact angles. However, also with the highest added amount of EHM, beeswax20/CNC1/EHM3, the contact angle is quite high, 109°. Thus, there is only a slight reduction of hydrophobicity with an increase in the EHM concentration up to 3 %. The high degree of hydrophobicity of the consolidant layers was maintained also in a humid environment.

Next, compositions with low amount of beeswax, 2 % and 5 %, together with 1 % CNC and 0.5 % or 1.0 % EHM were examined. Fig. 5b and c shows water contact angles of 118°, 116° 131° and 126° for beeswax2/CNC1/EHM0.5, beeswax2/CNC1/EHM1, beeswax5/CNC1/EHM0.5 and beeswax5/CNC1/EHM1, respectively. The results show that a higher beeswax content in the emulsion gives a higher degree of hydrophobicity to the consolidant layer, which is according to expectations. Without EHM the values were somewhat lower, 93° and 105° for beeswax2/CNC1 and beeswax5/CNC1, respectively. This result indicates that when the beeswax concentration in the emulsion is low, the addition of EHM enhances hydrophobicity compared to the beeswax/CNC Pickering emulsion alone. This is probably because EHM promotes the formation of a continuous layer with the beeswax/CNC microparticles. When the beeswax content is high, the microparticles become densely packed, ensuring pronounced hydrophobicity. However, at lower beeswax concentrations, the continuous layer becomes essential as it minimizes water penetration into the porous structure of the loosely packed microparticles.

Formulations with a low content of CNC (0.2 % and 0.5 %) and with an EHM content of 0.5 % were also investigated. The contact angles of the consolidant layers from the emulsions beeswax2/CNC0.2/EHM0.5 and beeswax5/CNC0.2/EHM0.5 gave water contact angles of 109° and 126°, respectively. Corresponding formulations without EHM, i.e. beeswax2/CNC0.2 and beeswax5/CNC0.2, gave contact angles of 109° and 115°, respectively. Thus, the effect on the hydrophobicity of small amounts of added EHM is not obvious.

The viscosity of the emulsions was investigated by a Brookfield viscometer. Three different beeswax contents, 2 %, 5 % and 20 %, were used while the CNC content was kept constant at 1 %. EHM was added in concentrations from 0 % to 3 %. As shown in Table 1, the viscosity of beeswax2/CNC1, beeswax5/CNC1 and beeswax20/CNC1 emulsions were 12.8 cP, 13.6 cP and 29.0 cP, respectively. Thus, an increasing amount of beeswax in the emulsion gave an increase in viscosity, as expected. However, even with the highest beeswax content the viscosity was deemed too low for the emulsion to be used as a consolidant for

**Table 1**
Viscosity of beeswax20/CNC1/EHM(0, 0.2, 0.5, 1, 2, 3), beeswax(2, 5)/CNC1/EHM(0.5, 1), beeswax(2, 5)/CNC1, CNC1/EHM(1, 2) and EHM(0.2 %, 0.5 %, 1 %, 2 %, 3 %).

| Formulations | Viscosity (cP) | Formulations | Viscosity (cP) |
|---|---|---|---|
| Beeswax2/CNC1[a] | 12.8 ± 0.1 | 3 % EHM | 36,933 ± 205 |
| Beeswax5/CNC1 | 13.6 ± 0.2 | Beeswax2/CNC1/EHM0.5 | 349.3 ± 1.5 |
| Beeswax20/CNC1 | 29.0 ± 0.2 | Beeswax5/CNC1/EHM0.5 | 349.7 ± 2.1 |
| Beeswax20/EHM1 | 47.9 ± 0.3 | Beeswax2/CNC1/EHM1 | 54,810 ± 165 |
| CNC1/EHM1 | 352.5 ± 0.5 | Beeswax5/CNC1/EHM1 | 68,200 ± 1479 |
| CNC1/EHM2 | 32,773 ± 23 | Beeswax20/CNC1/EHM0.2 | 2180 ± 20 |
| 0.2 % EHM | 60.8 ± 1.6 | Beeswax20/CNC1/EHM0.5 | 48,400 ± 400 |
| 0.5 % EHM | 83.2 ± 0.8 | Beeswax20/CNC1/EHM1 | 236,000 ± 2000 |
| 1 % EHM | 90.2 ± 0.8 | Beeswax20/CNC1/EHM2 | 667,333 ± 3055 |
| 2 % EHM | 10,640 ± 40 | Beeswax20/CNC1/EHM3 | 1,182,667 ± 11,015 |

[a] 2 wt% beeswax and 1 wt% CNC in water.

flaking encaustic paintings. Additions of EHM result in a very pronounced viscosity increase, as can be seen from Table 1. The interaction between EHM and beeswax/CNC is evident from the values. As an example, the viscosity of 1 % EHM is 90.2 cP and that of beeswax20/CNC1 is 29.0 cP; however, the viscosity after mixing, i.e. of beeswax20/CNC1/EHM1, is 236,000 cP. To verify the interactions, the viscosity of beeswax20/EHM1 and CNC1/EHM1 were also measured and showed 47.9 cP and 352.5 cP, respectively. Thus, the viscosity resulting from the interaction among all three components is significantly higher than that observed from the interaction between any two components.

Reducing the beeswax content from 20 % to 5 % and further to 2 %, decreased the viscosity of the dispersion from 236,000 cP to 68,200 cP (beeswax5/CNC1/EHM1) and to 54,810 cP (beeswax2/CNC1/EHM1), respectively. Reducing the EHM content from 1 % to 0.5 % resulted in a very pronounced drop in viscosity. Both beeswax2/CNC1/EHM0.5 and beeswax5/CNC1/EHM0.5 exhibited a viscosity of only 349 cP. Reducing the CNC content from 1 % to 0.5 % and 0.2 % gave viscosities so low that they could not be quantified with the viscometer.

Taken together, the results from the viscosity measurements provide clear evidence of the strong interaction between EHM, CNC and beeswax in the dispersion and that this interaction is concentration dependent, mainly through hydrophobic interaction. Subsequently, UV–Vis (ultraviolet-visible spectroscopy) was used to investigate the turbidity of a CNC dispersion at a low concentration of 0.1 % as a function of added EHM. The results are shown in Fig. S7, where the absorbance of EHM solutions at different concentrations is also included for comparison. Both the CNC absorbance vs. EHM concentration and the EHM absorbance at varying concentrations show a linear relationship, which could be expected in case of minor interactions. The data obtained supports the view that there is no significant interaction between EHM and CNC at low concentrations, explaining the almost undetectable viscosity of the low concentration dispersions such as beeswax0.5/CNC0.5/EHM0.5 and beeswax0.5/CNC0.2/EHM0.5. The very strong increase in viscosity when EHM is added to the beeswax/CNC system is most likely due to hydrophobic interactions between the hydrophobic side chains of EHM and the hydrophobic beeswax/CNC microparticles' surface. EHM acts as a crosslinker for the beeswax/CNC, just as it does for surfactant micelles in regular coatings formulations [37,38].

Furthermore, the results indicate that the viscosity of the dispersions is tunable by varying the amounts of the three components, beeswax, CNC and EHM. The higher the concentration, the stronger the interaction and the higher the viscosity. Fine-tuning of the viscosity of the consolidant is important because the optimal viscosity will vary with the application method - by brush or by injection through syringes, etc. - on the flaking painting layer.

The load-extension curves of single lap joints and average failure forces with different adhesives are shown in Figs. 6 and S8. The adhesive strength of beeswax/CNC/EHM dispersions was compared with the strength of the natural consolidant gelatin and the synthetic consolidant Aquazol (poly(2-ethyl-2-oxazoline)). Plain beeswax and plain EHM were also included as references. The curves show a nearly linear behavior and remain steady until the load reaches complete failure, which leads to delamination of the bonded area. Some of the samples, such as 2 % Aquazol, 3 % gelatin and 1 % EHM display a weak load force and shear strength of 40 N or below, which may be due to a combination of low concentrations and hydrophilic nature. A hydrophilic polymer is likely not to spread well between the smooth Masonite surface and the hydrophobic wax layer and without proper wetting and spreading the bond strength will be poor.

The 2 % EHM solution is thicker and shows a strength comparable with that of the beeswax20/CNC1 emulsion, giving a failure load of about 70 N. However, their shear strengths are still lower than that of hot beeswax. A significant increase in bonding strength was observed after including EHM in the formulation. Beeswax20/CNC1/EHM1 gave a failure load of 95 N, which is comparable to that of beeswax. The failure load of beeswax20/CNC1/EHM2 was higher, reaching 116 N. As can be seen, when the concentration of Aquazol was increased to 20 %, the failure load became even higher, 169 N. However, a very high bonding strength may not be optimal. For conservation of cultural heritage, the strength of a consolidant should be comparable to the strength of the substrate to avoid unnecessary additional stress on the artwork.

The water vapor transmission rate (WVTR) of different consolidants was evaluated and is shown in Figs. 6c and S9. Beeswax and Aquazol were selected as reference materials to represent hydrophobic and hydrophilic coatings, respectively, for comparison with the developed beeswax/CNC/EHM formulations. The uncoated Whatman filter paper initially exhibited a WVTR of 37.8 g/h•m$^2$, which decreased to 22.6 g/h•m$^2$ within the first 3–22 h. Over time, the WVTR gradually stabilized at around 21 g/h•m$^2$. The observed decrease in the beginning is attributed to the equilibration process when the dry samples were exposed to a humid environment. A similar trend was observed for all coated samples, except for the beeswax coated sample, where the pores of the paper were clogged and sealed by the beeswax layer. As a result, the sample exhibited a significantly lower WVTR. The Aquazol coated sample exhibited an initial WVTR of 26.4 g/h•m$^2$, which decreased to 15.1 g/h•m$^2$ before stabilizing at around 18 g/h•m$^2$. As a hydrophilic, non-porous coating, Aquazol facilitates water vapor transfer through chemical diffusion, absorbing water molecules from the high-humidity side and releasing them on the low-humidity side [42]. However, hydrophilic coatings may lose mechanical properties in humid environments. For the beeswax20/CNC1/EHM1 coating, the WVTR decreased from 31.9 g/h•m$^2$ to 20.2 g/h•m$^2$ before stabilizing at about 18 g/h•m$^2$, which was slightly higher than was obtained with the Aquazol coating. The beeswax2/CNC1/EHM1 coating demonstrated a WVTR range from 33.3 g/h•m$^2$ to 21.4 g/h•m$^2$ before stabilizing at around 20 g/h•m$^2$, showing the best WVTR performance, which is comparable with the uncoated Whatman filter paper. The beeswax/CNC/EHM formulations contain beeswax hollow microparticles, which provide channels for water vapor transfer while preventing external water from penetrating, thus exhibiting both water resistance and breathability.

### 3.3. *Evaluation of consolidation efficiency*

The color differences of various consolidants were measured on both encaustic mockup and Whatman filter paper (Fig. S10). As shown in Fig. 7a and Table S2, the CIE color coordinates (L*, a*, b*) represent the

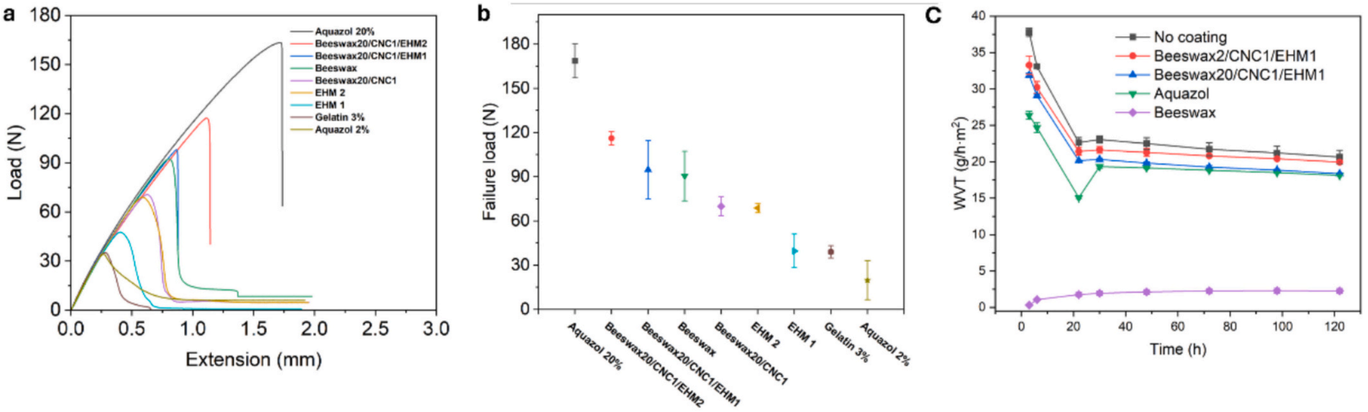

**Fig. 6.** (a) Force-extension curves of the lap-shear test; (b) average failure load of various materials; (c) water vapor transmission rate (WVTR) of Whatman filter paper before and after coating with beeswax, 20 % Aquazol, beeswax20/CNC1/EHM1 and beeswax2/CNC1/EHM1.

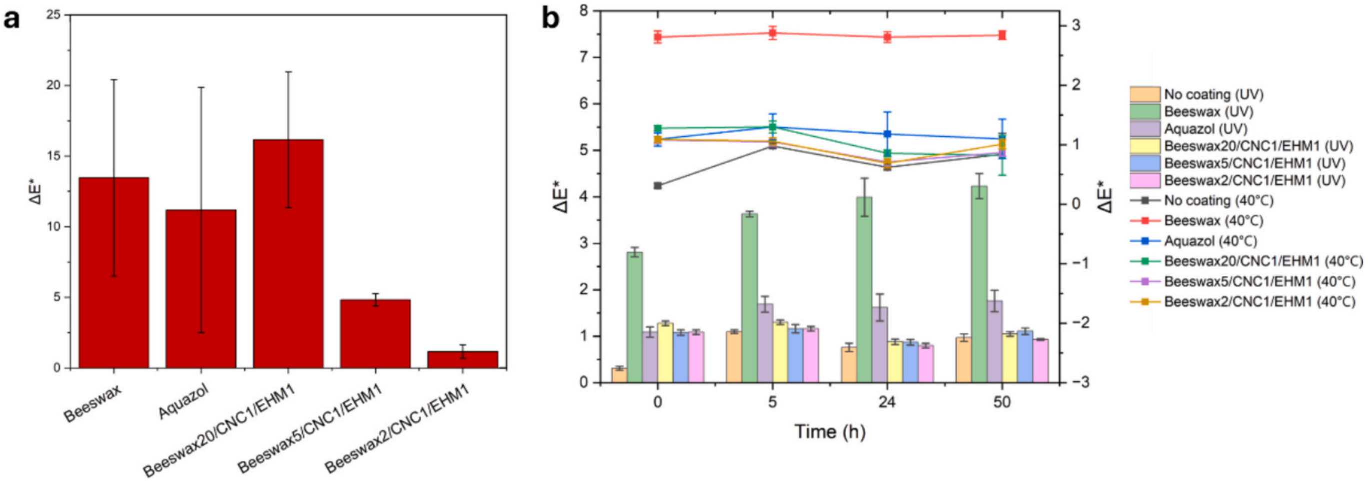

**Fig. 7.** The color change (ΔE*) of (a) encaustic mockup before and after coating with beeswax, 20 % Aquazol, beeswax20/CNC1/EHM1, beeswax5/CNC1/EHM1, beeswax2/CNC1/EHM1; (b) UV light aging and temperature effect on the above consolidants.

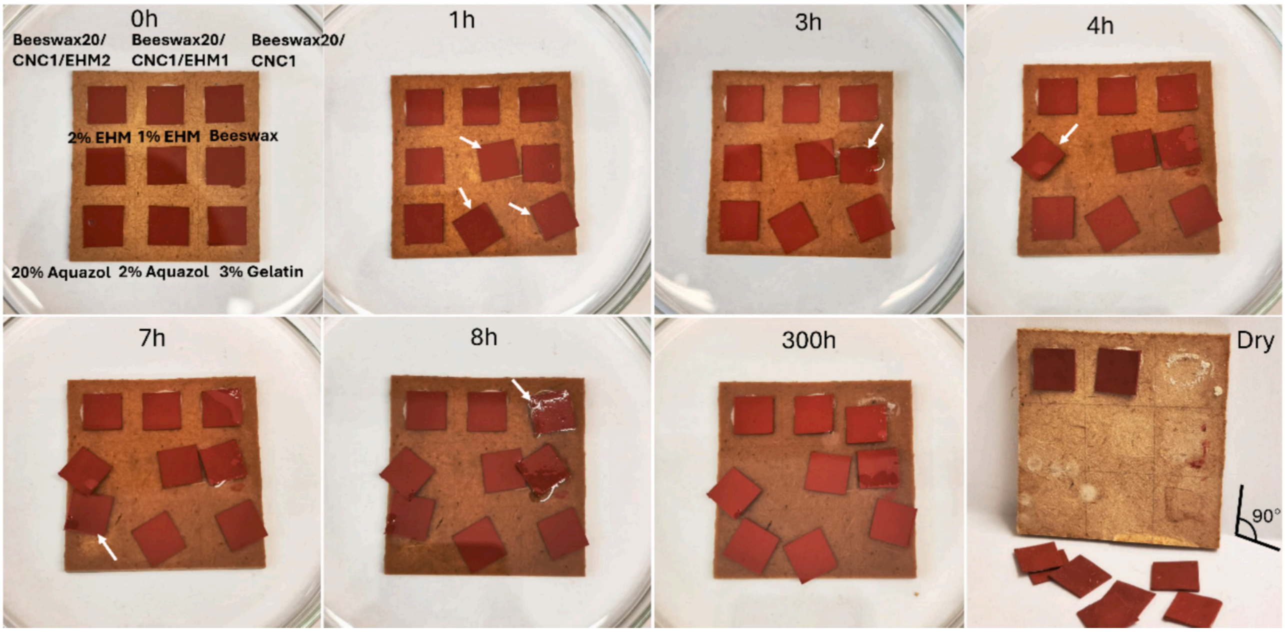

**Fig. 8.** Images of mockups immersed in a Petri dish filled with water over time. The composition of the formulations is given on the top, left picture.

color values in the color space, while ΔE* indicates the overall color change of the consolidants applied to the mockup surface. From the results, the ΔE* values for beeswax, Aquazol, beeswax20/CNC1/EHM1, beeswax5/CNC1/EHM1 and beeswax2/CNC1/EHM1 were 13.5, 11.2, 16.2, 4.8 and 1.2, respectively. Aquazol exhibited a glossy appearance and showed significant color variations depending on the measuring angle. The beeswax20/CNC1/EHM1 formulation appeared whitish when applied to the red encaustic surface. The high beeswax content formulation is more suitable for adhesion of flaking paint layers rather than as a surface coating. Reducing the beeswax content from 20 % to 2 % significantly reduced the impact of the hydrophobic consolidant on the appearance of the mockup. To assess the color stability of the consolidants before and after aging, a uniform layer was applied to a flat Whatman paper surface. As shown in Fig. 7b, the ΔE* values of the beeswax/CNC/EHM consolidants were lower than those of beeswax and Aquazol, making the color change nearly imperceptible to the human eye. Additionally, after 50 h of UV aging, only beeswax showed a slight increase in ΔE*. No significant ΔE* changes were observed in any of the consolidants after 50 h of aging at 40 °C.

In order to investigate the water resistance of the films from the beeswax20/CNC1/EHM1 and beeswax20/CNC1/EHM2 emulsions, mockups were prepared by bonding paint layer pieces on Masonite support with various adhesives. The paint layer was composed of a beeswax binder and red ochre pigment to simulate an encaustic painting. The mockup was immersed in a petri dish filled with water. Fig. 8 shows the flaking of the samples over time. As can be seen, the samples bonded with 3 % gelatin, 2 % Aquazol, and 1 % EHM detached from the Masonite during the first hour, most likely as a result of the hydrophilic nature of the binders and the relatively low concentration. After 3 h, the beeswax bonded sample flaked off. The sample bonded with 2 % EHM came off after 4 h and the one with 20 % Aquazol after 7 h. Comparison of the results with 2 % and 20 % Aquazol shows that a higher polymer concentration gives better adhesion in water.

The sample bonded with the beeswax20/CNC1 emulsion flaked off after 8 h while the samples bonded with the two beeswax20/CNC1/EHM emulsions remained on the Masonite for the entire test period of 300 h. Their water resistance was evidently much higher than that obtained with commonly used consolidants such as gelatin and Aquazol. This is important for the consolidation of objects that are kept in humid environments. It is remarkable that this high degree of water resistance, as well as pronounced hydrophobicity of the applied layer, as discussed above, is obtained with an adhesive that is water-based and free from organic volatile components.

An evaluation of the performance of the consolidants under varying humidity was performed by DMA (dynamical mechanical analysis), using paper as a substrate. Paper was deemed to be a good proxy of typical substrate of encaustic painting. A super glue was used as a moisture-inert reference compound and Aquazol was employed as a highly water-sensitive reference. As shown in Fig. 9a, the consolidant formulations beeswax20/CNC1/EHM1 and beeswax20/CNC1/EHM2 show a behavior similar to that of super glue. The storage modulus shows that both the consolidants and the super glue soften with increasing RH. This is most likely due to softening of the paper caused by plasticization by water. Aquazol, on the other hand, becomes tougher and more difficult to deform at 60 % RH but softens completely at 80 % RH. The toughening is likely related to better contact between the paper and the adhesive when both components have been plasticized with water. The softening at 80 % is probably a result of a glass transition of the Aquazol as it takes up enough water. Aquazol has been shown to have a $T_g$ close to room temperature at ambient conditions [43]. This suggestion is supported by the loss modulus peaking as the RH ramps from 60 to 80 % RH (Fig. S11), typical of a glass transition.

As the DMA instrument records the length of the sample, it is possible to monitor the extension of the material; however, as the static force changes throughout the experiment, these results are not as informative as they would have been with an unchanging static force. As shown in Fig. 9b, all materials elongate upon increasing the moisture content, but the elongation of the Aquazol sample is exceptionally large, most likely due to a drawing out of the joint. The two consolidants behave like the super glue, indicating that the elongation of these samples is mainly the result of a softening of the paper.

## 4. Conclusion

We here report an approach to combine CNC stabilized Pickering emulsions of beeswax with EHM for consolidation of deteriorated encaustic paintings. The formulations are entirely composed of eco-friendly materials, beeswax, cellulose nanocrystals and a surface active cellulose derivative and contain no volatile components. They are easy to prepare and can be used at room temperature. The Pickering emulsion displays a microsphere structure with droplet inclusion, and the microspheres' size is governed by the concentration of beeswax in the formulation. The viscosity of the dispersion is governed by the amount of EHM. The dried film is highly hydrophobic, with a water contact angle of about 130°, which is beneficial to have similar property as the original artefact. This hydrophobicity remained stable under humid conditions while allowing efficient water vapor transfer, ensuring high breathability. The mechanical and water resistance tests conducted on mockups showed that the dried films have very good adhesive strength and excellent water resistance.

Since the components of the beeswax dispersion are all based on natural raw materials and of similar nature as the encaustic painting's original materials, i.e. lignocellulosic materials and beeswax, the risk of incompatibility between the consolidant and the painting, which is

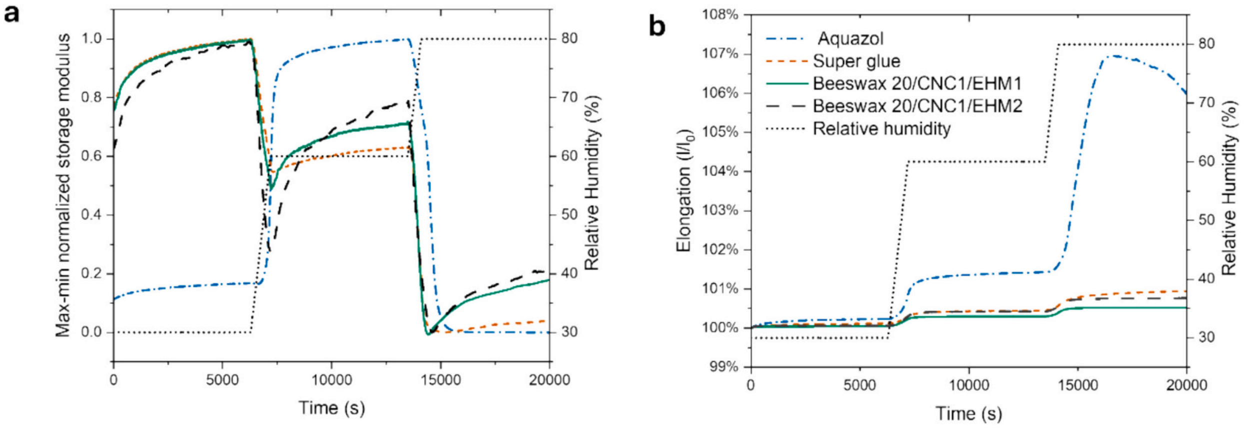

**Fig. 9.** (a) Max-min normalized storage modulus and (b) elongation, as a function of time, with the relative humidity displayed on the right axes.

sometimes encountered with consolidants based on synthetic polymers, is eliminated. In summary, this study presents a novel, efficient, eco-friendly, and humidity-resistant consolidant for the cultural heritage conservation field that should be of particular value for encaustic paintings.

## CRediT authorship contribution statement

**Yiming Jia:** Writing – original draft, Visualization, Investigation, Data curation, Conceptualization. **Åke Henrik-Klemens:** Writing – original draft, Investigation, Data curation. **Michael Persson:** Writing – review & editing. **Krister Holmberg:** Writing – review & editing, Supervision. **Romain Bordes:** Writing – review & editing, Supervision, Conceptualization.

## Declaration of competing interest

The authors declare that they have no known competing financial interests or personal relationships that could have appeared to influence the work reported in this paper.

## Acknowledgments

This work was performed within the European Union project GREen ENdeavor in Art ResToration (GREENART, Grant Agreement Number: 101060941).

## Appendix A. Supplementary data

Supplementary data to this article can be found online at https://doi.org/10.1016/j.ijbiomac.2025.144085.

## References

[1] E. Bosco, A.S.J. Suiker, N.A. Fleck, Moisture-induced cracking in a flexural bilayer with application to historical paintings, Theor. Appl. Fract. Mec. 112 (2021) 102779.

[2] G.J.A. Eumelen, E. Bosco, A.S.J. Suiker, J.J. Hermans, Chemo-mechanical model for degradation of oil paintings by amorphous and crystalline metal soaps, Eur. J. Mech. A-Solid. 97 (2023) 104827.

[3] A. Colombo, F. Gherardi, S. Goidanich, J.K. Delaney, E.R. de la Rie, M.C. Ubaldi, L. Toniolo, R. Simonutti, Highly transparent poly(2-ethyl-2-oxazoline)-TiO$_2$ nanocomposite coatings for the conservation of matte painted artworks, RSC Adv. 5 (2015) 84879–84888.

[4] A. Pataki-Hundt, E. Hummert, Colour stability of natural adhesives–light ageing of adhesive films and colour changes of pigment layers after aerosol application, Int. J. Preserv. Lib. Arch. Mater. 37 (2) (2016) 137–156.

[5] C.A. Del Grosso, J.A. Poulis, E.R. de la Rie, The photo-stability of acrylic tri-block copolymer blends for the consolidation of cultural heritage, Polym. Degrad. Stab. 159 (2019) 31–42.

[6] E. Carretti, L. Dei, Physicochemical characterization of acrylic polymeric resins coating porous materials of artistic interest, Prog. Org. Coat. 49 (3) (2004) 282–289.

[7] R. Giorgi, M. Baglioni, D. Berti, P. Baglioni, New methodologies for the conservation of cultural heritage: micellar solutions, microemulsions, and hydroxide nanoparticles, Acc. Chem. Res. 43 (6) (2010) 695–704.

[8] K. Soppa, A. Hoess, M. Läuchli, S. Meyer, T. Geiger, N.C. Scherrer, S. Zumbühl, T. Haupt, in: K.J. Van den Berg, I. Bonaduce, A. Burnstock, B. Ormsby, M. Scharff, L. Carlyle, G. Heydenreich, K. Keune (Eds.), In Conservation of Modern Oil Paintings, Springer, Cham, 2019, pp. 597–606.

[9] J. Zhu, P. Zhang, J. Ding, Y. Dong, Y. Cao, W. Dong, X. Zhao, X. Li, M. Camaiti, Nano Ca(OH)$_2$: a review on synthesis, properties and applications, J. Cult. Herit. 50 (2021) 25–42.

[10] E. Galvagno, E. Tartaglia, M. Stratigaki, C. Tossi, L. Marasco, F. Menegazzo, C. Zanardi, F. Omenetto, C. Coletti, A. Traviglia, M. Moglianett, Present status and perspectives of graphene and graphene-related materials in cultural heritage, Adv. Funct. Mater. 34 (2024) 2313043.

[11] P. Baglioni, D. Chelazzi, R. Giorgi, G. Poggi, Colloid and materials science for the conservation of cultural heritage: cleaning, consolidation, and deacidification, Langmuir 29 (17) (2013) 5110–5122.

[12] D. Chelazzi, G. Poggi, Y. Jaidar, N. Toccafondi, R. Giorgi, P. Baglioni, Hydroxide nanoparticles for cultural heritage: consolidation and protection of wall paintings and carbonate materials, J. Colloid Interface Sci. 392 (2013) 42–49.

[13] I. Franco-Castillo, L. Hierro, J.M. de la Fuente, A. Seral-Ascaso, S.G. Mitchell, Perspectives for antimicrobial nanomaterials in cultural heritage conservation, Chem 7 (3) (2021) 629–669.

[14] A.P. Kanth, A.K. Soni, Application of nanocomposites for conservation of materials of cultural heritage, J. Cult. Herit. 59 (2023) 120–130.

[15] J. Zhu, X. Li, Y. Zhang, J. Wang, B. Wei, Graphene-enhanced nanomaterials for wall painting protection, Adv. Funct. Mater. 28 (2018) 1803872.

[16] A. Casini, D. Chelazzi, R. Giorgi, Jin Shofu starch nanoparticles for the consolidation of modern paintings, ACS Appl. Mater. Interfaces 13 (2021) 37924–37936.

[17] R. Giorgi, L. Dei, M. Ceccato, C. Schettino, P. Baglioni, Nanotechnologies for conservation of cultural heritage: paper and canvas deacidification, Langmuir 18 (21) (2002) 8198–8203.

[18] A.C. Egil, B. Ozdemir, S.K. Gunduz, M. Altıkatoglu-Yapaoz, Y. Budama-Kilinc, E. Mostafavi, Chitosan/calcium nanoparticles as advanced antimicrobial coating for paper documents, Int. J. Biol. Macromol. 215 (2022) 521–530.

[19] S. Li, J. Tang, L. Jiang, L. Jiao, Conservation of aged paper using reduced cellulose nanofibrils/aminopropyltriethoxysilane modified CaCO$_3$ particles coating, Int. J. Biol. Macromol. 255 (2024) 128254.

[20] M. Bicchieri, F. Valentini, F. Pascalicchio, M.L. Riccardi, P. Colaizzi, C. Del Re, M. Talamo, The solution to an unresolved problem: newly synthesised nanocollagen for the preservation of leather, J. Cult. Herit. 33 (2018) 1–9.

[21] J. Zhang, Y. Li, D. Ke, C. Wang, H. Pan, K. Chen, H. Zhang, Modified lignin nanoparticles as potential conservation materials for waterlogged archaeological wood, ACS Appl. Nano Mater. 6 (13) (2023) 12351–12363.

[22] K. Kolman, O. Nechyporchuk, M. Persson, K. Holmberg, R. Bordes, Combined nanocellulose/nanosilica approach for multiscale consolidation of painting canvases, ACS Appl. Nano Mater. 1 (5) (2018) 2036–2040.

[23] O. Nechyporchuk, K. Kolman, A. Bridarolli, M. Odlyha, L. Bozec, M. Oriola, G. Campo-Francés, M. Persson, K. Holmberg, R. Bordes, On the potential of using nanocellulose for consolidation of painting canvases, Carbohydr. Polym. 194 (2018) 161–169.

[24] A. Bridarolli, M. Odlyha, G. Burca, J.C. Duncan, F.A. Akeroyd, A. Church, L. Bozec, Controlled environment neutron radiography of moisture sorption/desorption in nanocellulose-treated cotton painting canvases, ACS Appl. Polym. Mater. 3 (2) (2021) 777–788.

[25] J. Cuní, P. Cuní, B. Eisen, R. Savizky, J. Bové, Characterization of the binding medium used in Roman encaustic paintings on wall and wood, Anal. Methods 4 (3) (2012) 659–669.

[26] S. Hosseini, Z. Mousavi, D. McClements, Beeswax: a review on the recent progress in the development of superhydrophobic films/coatings and their applications in fruits preservation, Food Chem. 424 (2023) 136404.

[27] L. Angelova, in: R. Ballestriero, O. Burke, F.M. Galassi (Eds.), In Ceroplastics: The Art of Wax, L'Erma Di Bretschneider, Roma, 2019, pp. 169–183.

[28] R. Ploeger, C.W. McGlinchey, E.R. de la Rie, Original and reformulated BEVA® 371: composition and assessment as a consolidant for painted surfaces, Stud. Conserv. 60 (4) (2015) 217–226.

[29] L. Bianco, M. Avalle, A. Scattina, P. Croveri, C. Pagliero, O. Chiantore, A study on reversibility of BEVA® 371 in the lining of paintings, J. Cult. Herit. 16 (2015) 479–485.

[30] G. Tarantola, E. Medri, A. Splendore, F. Lo Russo, C. Matteucci, M. Minelli, Liquid foam-ethyl vinyl acetate adhesive systems for lining process of paintings: prospects of a user-friendly, harmless alternative to conventional products, Polymers 15 (7) (2023) 1741.

[31] D.G. Ortiz, C. Pochat-Bohatier, J. Cambedouzou, M. Bechelany, P. Miele, Current trends in Pickering emulsions: particle morphology and applications, Engineering 6 (4) (2020) 468–482.

[32] F. Heidari-Dalfard, S. Tavasoli, E. Assadpour, R. Miller, S.M. Jafari, Surface modification of particles/nanoparticles to improve the stability of Pickering emulsions: a critical review, Adv. Colloid Interf. Sci. 336 (2024) 103378.

[33] G. Cavallaro, S. Milioto, L. Nigamatzyanova, F. Akhatova, R. Fakhrullin, G. Lazzara, Pickering emulsion gels based on halloysite nanotubes and ionic biopolymers: properties and cleaning action on marble surface, ACS Appl. Nano Mater. 2 (5) (2019) 3169–3176.

[34] L. Lisuzzo, T. Hueckel, G. Cavallaro, S. Sacanna, G. Lazzara, Pickering emulsions based on wax and halloysite nanotubes: an ecofriendly protocol for the treatment of archeological woods, ACS Appl. Mater. Interfaces 13 (1) (2020) 1651–1661.

[35] I. Capron, O.J. Rojas, R. Bordes, Behavior of nanocelluloses at interfaces, Curr. Opin. Colloid Interface Sci. 29 (2017) 83–95.

[36] A. Samanta, O. Nechyporchuk, R. Bordes, Wet spinning of strong cellulosic fibres with incorporation of phase change material capsules stabilized by cellulose nanocrystals, Carbohydr. Polym. 312 (2023) 120734.

[37] K. Thuresson, B. Lindman, Effect of hydrophobic modification of a nonionic cellulose derivative on the interaction with surfactants. Phase behavior and association, J. Phys. Chem. B 101 (1997) 6460–6468.

[38] B. Kronberg, K. Holmberg, L. Björn (Eds.), Surface Chemistry of Surfactants and Polymers, John Wiley & Sons, 2014, pp. 278–282.

[39] M. Miguel, A.I. Barros, F.M. Nunes, A novel, direct, reagent-free method for the detection of beeswax adulteration by single-reflection attenuated total reflectance mid-infrared spectroscopy, Talanta 107 (2013) 74–80.

[40] A. Gao, H. Chen, J. Tang, K. Xie, A. Hou, Efficient extraction of cellulose nanocrystals from waste Calotropis gigantea fiber by $SO_4^{2-}/TiO_2$ nano-solid superacid catalyst combined with ball milling exfoliation, Ind. Crop. Prod. 152 (2020) 112524.

[41] A. Dinker, M. Agarwal, G.D. Agarwal, Experimental assessment on thermal storage performance of beeswax in a helical tube embedded storage unit, Appl. Therm. Eng. 111 (2017) 358–368.

[42] Y. Chang, F. Liu, Review of waterproof breathable membranes: preparation, performance and applications in the textile field, Materials 16 (15) (2023) 5339.

[43] K. Kelly, J. Herrmann, A. Chipman, A. Davis, Y. Khan, S. Loew, K. Danzis, T. Ohanyana, L. Varga, A. Witty, M. Youket, Heat- and solvent-set repair tissues, J. Am. Inst. Conserv. 61 (1) (2022) 24–54.